Electronic properties of the generalized Fibonacci lattices: energy spectrum and wavefunction

1992 J. Phys.: Condens. Matter 4 8187

(http://iopscience.iop.org/0953-8984/4/42/008)

J. Phys.: Condens. Matter 4 (1992) 8187–8202. Printed in the UK

Electronic properties of the generalized Fibonacci lattices: energy spectrum and wavefunction

G Y Oh, C S Ryu and M H Lee
Department of Physics, Seoul National University, Seoul 151-742, Korea

Received 20 December 1991, in final form 2 June 1992

Abstract. We study the electronic properties of a one-dimensional diagonal tight-binding model with potentials $\{V_n\}$ arranged in generalized Fibonacci (GF) sequences. Using the negative-eigenvalue theorem, we calculate the density of states (DOS). The DOS and the V dependence of energy spectra for silver-mean (SM) and copper-mean (CM) series clearly show distinctive features. The relation of the energy spectral feature to the geometry of the underlying lattices is emphasized. Various states of the CM lattice are examined in detail by means of wavefunctions, resistances and a multifractal analysis. Critical states are characterized both by scaling transformations and by multifractal behaviours. We find that states with a strongly localized wavefunction under a given system size exhibit additional wavepackets with increasing system size. This shows that the localized behaviour of allowed states is a feature of the finite size of the system, and implies the absence of strongly localized states in a system of infinite size.

1. Introduction

Since the discovery of the quasicrystalline phase [1] much attention has been devoted to the study of quasiperiodic systems. The Fibonacci lattice, a one-dimensional version of a quasicrystal, has most widely been studied [2–8], and it is well established that the energy spectra form a Cantor set with Lebesgue measure zero [9] and the corresponding states are critical. Unusual properties of quasiperiodic systems, as well as the possibility of the realization of aperiodic superlattices by means of epitaxial-growth techniques [10], have stimulated the investigations of other kinds of deterministically aperiodic structures such as Thue–Morse [11], circle [12, 13], Rudin–Shapiro [13], period-doubling [14] and hierarchical [15–17] systems. A kind of GF lattice has also been introduced and studied extensively [18–29].

As in the cases of ordinary Fibonacci and Thue–Morse lattices, the trace-map approach has been used as a major tool in current research into the physical properties of GF lattices [18–21, 25–29]. This approach makes it easy to calculate the energy spectrum and to examine the properties of the states corresponding to allowed energies at any size of the system. Gumbs and Ali [18] have derived trace maps for several kinds of lattices to find that some of them are volume non-preserving and non-invertible unlike the trace map of the ordinary Fibonacci lattice. Kolář and Ali [20] have studied the attractors of volume non-preserving trace maps to illustrate the coexistence of regular Bloch-like and Cantor-like energy spectra. You *et al* [21] have independently derived a unified trace map to study diagonal and off-diagonal tight-binding models, and showed that the energy spectra are Cantor-like

0953-8984/92/428187+16$04.50

ones. Other kinds of approaches have also been tried. Severin and Riklund [22] have calculated the Fourier spectrum of GF lattices to classify the lattices into two classes depending on the spectral properties, and illustrated that the ordinary Fibonacci lattice is much more like the members of the $(n > 1, m = 1)$ class than those of the $(n = 1, m > 1)$ class. They have also analyzed one of the lattices (the nickel-mean lattice) to obtain numerically localized, critical and extended wavefunctions [23]. Chakrabarti and Karmakar [24] have calculated local and average Green functions of GF lattices by using an exact renormalization-group (RG) method to classify the lattices into two groups depending on their energy spectral properties, and illustrated that one of the groups has critical eigenstates while the other has some extended states.

It is well known that the Thue–Morse lattice has a singular continuous Fourier spectrum [30], which can be thought of as a link between quasiperiodic and disordered ones. On the other hand, there exist extended states belonging to Bloch-like energy spectra, which suggests that the electronic structure is intermediate between periodic and quasiperiodic ones. A similar situation holds for a class of GF lattices. The existence of extended states in a class of GF lattices is well known [20,23,24,32], while the aperiodicity of the class is known to be intermediate between quasiperiodic and disordered systems [22,25,31] even though there is no proof whether the Fourier spectrum of the class is singular continuous or not. This shows that further study of GF lattices is needed to understand the above seemingly inconsistent results between the geometrical characteristics (Fourier spectra) and energy spectral properties of the lattices in a consistent way. Note that most attention, in the existing literature, has been paid to the spectral properties, and much less attention has been paid to wavefunctions, except for [18,29,32]. Note also that the aperiodicity of a class of GF lattices may suggest the existence of localized states, and there exist some claims of the existence of localized states in certain cases of GF lattices [18,23,32].

In this paper, we study the relation of the energy spectral properties to the geometry of the underlying lattices as well as the characteristics of allowed states of a certain class of GF lattices. We also examine whether localized states can exist in the present model. The outline of the paper is the following. In section 2, we consider the global properties of the energy spectrum of GF lattices, especially in connection with the geometrical characteristics of the lattices. In section 3, the states of the CM lattice are examined by means of wavefunctions, resistances and a multifractal analysis. The possibility of the localization of the wavefunctions is also examined. Section 4 is devoted to a brief summary.

2. Global properties of GF lattices: geometry and energy spectrum

In the following, we consider a diagonal tight-binding model

$$\psi_{n+1} + \psi_{n-1} + V_n \psi_n = E\psi_n \tag{1}$$

where $\{V_n\}$ takes two values V_A and V_B arranged in the GF sequences defined by the recursion relation [20]

$$S_{l+1} = S_l^n S_{l-1}^m \qquad \text{with} \quad S_0 = \{B\} \quad S_1 = \{A\} \tag{2}$$

where l, n and m are positive integers. The substitution rule for the sequence equivalent to (2) is given by $(B, A) \rightarrow (A, A^n B^m)$, and the GF number F_{l+1} in the $(l+1)$th generation sequence S_{l+1} is given by the recursion relation

$$F_{l+1} = nF_l + mF_{l-1} \qquad F_0 = F_1 = 1. \tag{3}$$

The incommensurability and the ratios of A to B are given by

$$\sigma(n,m) = \lim_{l\to\infty} \frac{F_l}{F_{l-1}} = \tfrac{1}{2}[n + (n^2+4m)^{1/2}] \tag{4}$$

$$\tau(n,m) = \lim_{l\to\infty} \frac{N_l(A)}{N_l(B)} = \frac{1}{m}\sigma(n,m). \tag{5}$$

Here, the values of $\sigma(n,m)$ for $(n,m) = (1,1)$, $(2,1)$, $(3,1)$, $(1,2)$ and $(1,3)$ are golden mean (σ_G), silver mean (σ_S), bronze mean (σ_B), copper mean (σ_C) and nickel mean (σ_N) respectively, named after Gumbs and Ali [18]. By using the incommensurability, F_l can be written in a closed form as follows:

$$F_l = \frac{1}{\sigma_+ - \sigma_-}[(1-\sigma_-)\sigma_+^l + (\sigma_+ - 1)\sigma_-^l] \tag{6}$$

where σ_+ is $\sigma(m,n)$ and σ_- is given by $-m/\sigma_+$. Note that the CM lattice with $\sigma_C = 2$, which will be considered in detail in the following, does not mean periodic nor quasiperiodic. Note also that the statistics of letters A and B depends on the initial condition of the recursion relation [29]†. In the following we consider only the case of the initial condition given by (2). Let us classify the lattices into two series as in [19,22], the SM($n > 1, m = 1$) and the CM($n = 1, m > 1$) series, and consider the geometrical characteristics of the lattices.

In the SM series, $\sigma(n,1)$ belongs to the positive solutions of the following quadratic equation and is always irrational for any value of n:

$$\sigma^2 - n\sigma - 1 = 0. \tag{7}$$

Furthermore, letter B always exists in isolation while letter A exists in clusters with $[\sigma(n,1)] = n$ or $[\sigma(n,1)+1] = (n+1)$ letters, where the symbol $[x]$ denotes the greatest integer not exceeding x. On these bases, it is easy to consider that the sequences of the SM series are closely related to a 'p sequence' sometimes referred to as a 'Beatty sequence' [33]:

$$p_j(u,w) = \left[\frac{j+1}{u} + w\right] - \left[\frac{j}{u} - w\right]. \tag{8}$$

† After the submission of this paper we were kindly informed of the paper by Severin *et al* [29], which deals with a model similar to ours. In their paper the authors have performed an analytical study of the nature of the states in the CM lattice with two kinds of initial conditions to prove the existence of extended states (similar to the recurrent wavepackets in our model or *lattice-like* wavefunctions in [37]). A model with initial conditions $S_0 = A$, $S_1 = BA$ has $\sigma = \tau = 2$ and can be described by the substitution rule $(A, B) \rightarrow (BA, AA)$, which are different from ours ($\sigma = 2\tau = 2$ and $(A, B) \rightarrow (AB^2, A)$). However, the lattice structure resembles ours if a single B element in the model is replaced by BB. From this resemblance one may expect similar physical properties between the two models. The similar properties can easily be explained qualitatively by using the approximate RG method [3,5,38]. Note that the wavefunction for the fixed point in the text corresponds to a class that they treated. A paper by Miyazaki and Inoue [29] also deals with GF lattices with arbitrary initial conditions.

The sequence becomes periodic if u is a rational number, and quasiperiodic if u is an irrational number. The numbers of 1 and 0 in the first jth position of the sequence are

$$N_1 = \left[\frac{j+1}{u} + w\right] \sim \frac{j}{u} + O(1) \tag{9}$$

$$N_0 = \left[\frac{j+1}{v} + w\right] \sim \frac{j}{v} + O(1) \tag{10}$$

where $1/u + 1/v = 1$. The ratio of ones to zeros in the infinite limit of the sequence becomes

$$\tilde{\sigma} \equiv \lim_{j\to\infty} \frac{N_1}{N_0} = \frac{v}{u} = \frac{1}{u-1}. \tag{11}$$

Setting (11) equal to (5), u can be expressed in terms of n as follows:

$$u \equiv u_n = \tfrac{1}{2}[(n^2+4)^{1/2} - n + 2]. \tag{12}$$

It is easy to check that the p sequence with u_n and a suitable value of shift parameter w produces the same sequence with (2) for a given n if we match 1(0) with $A(B)$. Thus it can be said that the SM series is a class of quasiperiodic structures described by (8) with different u. From (12), the relation of u between different n can be written as follows:

$$u_{n+1} = f(u_n) \tag{13}$$

where the transformation function $f(u)$ can be easily expressed from (12). It is interesting to note that Odagaki and Aoyama [34], who have studied one-dimensional periodic and quasiperiodic sequences generated by a projection method, found hyperinflation rules which relate sequences characterized by different u, and illustrated that the physical properties, such as diffraction patterns and the product of transfer matrices, have self-similar structures. They argued that self-similarities in physical properties are due to inflation symmetry. Following their arguments, one can expect that there may exist an inflation symmetry satisfying (13), although it does not seem to be easy to find the inflation rules, and thus expect that properties such as the diffraction pattern have self-similarity. Fourier spectra obtained by Severin and Riklund [22] agree well with this expectation.

The geometry of the CM series is quite different from that of the SM series. There is no isolated B letter in the sequence. The letter B always exists in clusters of m letters while the letter A exists isolated or in clusters of $(m+1)$ letters, and it seems to be difficult to describe the sequence by a quasiperiodic sequence such as (8). Thus physical properties such as the Fourier spectrum and the energy spectrum of the CM series may be different from those of the SM series.

In order to understand the energy spectral properties of the GF lattices we calculated the density of states (DOS) by using the negative-eigenvalue theorem [35]. To confirm the result of the DOS and to know the localization behaviours of allowed states, we also calculated the inverse localization length defined by $\xi = \ln(1+R)/N$ as a function of E, where R is the resistance obtained from the Landauer

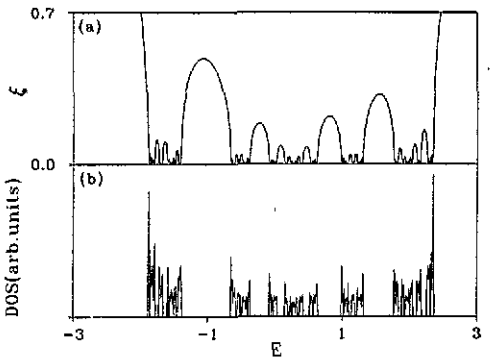

Figure 1. Energy dependence of ξ and the DOS of the SM lattice ($n = 2$, $m = 1$) with $V_A = -V_B = 0.6$ and $l = 10 (N = 3363)$. Self-similarities in ξ and the DOS are clearly shown.

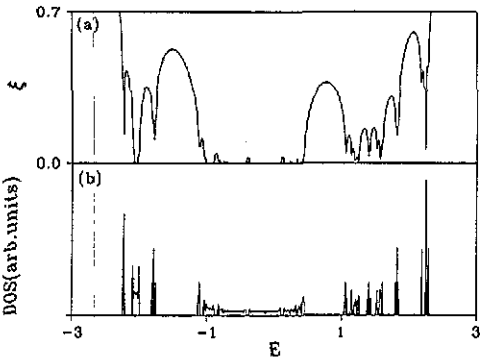

Figure 2. Energy dependence of ξ and the DOS of the CM lattice ($n = 1$, $m = 2$) with $V_A = -V_B = 0.6$ and $l = 12 (N = 2731)$. Self-similarities are not clear.

formula [36]. Figures 1 and 2 show ξ and the DOS for typical examples of the SM series ($n = 2, m = 1$; SM lattice) and the CM series ($n = 1, m = 2$; CM lattice) respectively. We take N to be 3363 and 2731 which are the tenth and the twelfth periodic approximants of the systems.

As shown in the figures, ξ and the DOS of the two lattices show different behaviours. In figure 1, self-similarities in ξ and the DOS are clearly shown. Moreover, one can see that the energies of the allowed states have small widths compared with those of figure 2, and one can expect that the total bandwidth of the SM lattice will eventually shrink to zero forming a Cantor set in the limit of infinite system size. In fact, we calculated the size dependence of the total bandwidth B_l for both SM and CM series. For the SM series, we obtained $B_l \sim F_l^{-\delta}$ where the exponent δ is independent of l, which agrees with the result of Wijnands [37].

On the other hand, self-similarities in figure 2 are less clear, and the energy spectrum contains broad subbands with negligibly small ξ, in which the states are expected to exhibit extended behaviours [20,23,24,32]. The size dependence of B_l for the CM lattice is different from that of the SM lattice. We could not obtain the l-independent exponent δ, which seems to be the existence of dense subset in the spectrum. Besides, there exist large values of ξ corresponding to the allowed states, in which localized behaviours of the states are expected. We treat the behaviours of these states in section 3. We want to comment here that figure 2 gives a qualitative picture with which to understand the results of diffraction patterns and energy spectra. From this figure and the study to be discussed in section 3, one can see that the allowed states of the CM lattice exhibit either extended or localized behaviour depending on the values of ξ and the DOS, which in turn reflects the Bloch-like energy spectra and the aperiodicity of the lattice.

The global structure of SM and CM lattices has six and five main subbands respectively. The origin of the global structure can be easily understood by means of an approximate RG approach [3,5,38]. For the regime where the approximate RG method holds ($1/|V_A - V_B| \ll 1$), the constructing elements for the SM and CM lattices are given by $\{B, AA, AAA\}$ and $\{BB, A, AAA\}$ respectively. In each case, the constructing elements give six energies which give rise to the global structure. But, in the case of the CM lattice, the energy coming from the monatomic

element (A) and one of the three energies coming from the triatomic element (AAA) are nearly degenerate in the lowest-order approximation [39], which results in the five main subband structure. Though the argument of the approximate RG method is appropriate for the large-V regime, the continuity of E–V phase diagrams in figures 3(a) and (b) insures that the global band structure is easily understood for any value of V.

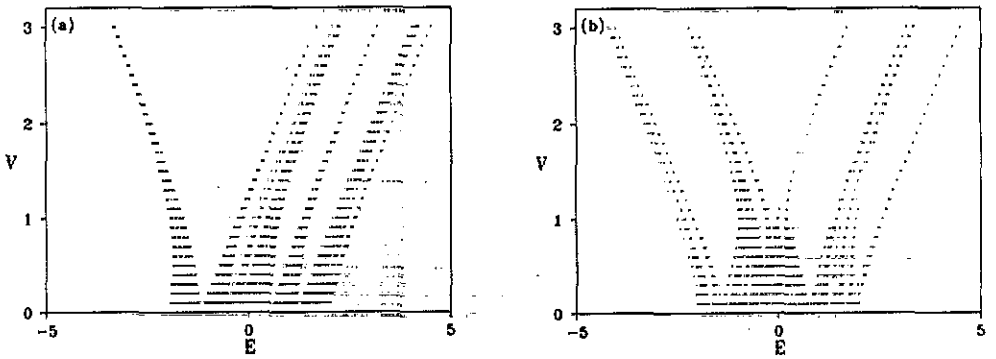

Figure 3. V dependence of the energy spectrum for (a) the SM lattice with $N = 239$, (b) the CM lattice with $N = 171$.

One of the interesting features of GF lattices lies in the V dependence of the energy spectra. If a lattice were periodic with $V_A = V_B = V$, the energy spectrum would merely shift to a higher energy region without changing the bandwidth as the potential V increases. However, the situation for non-periodic lattices becomes quite different. Figures 3(a) and 3(b) show the V dependence of the energy spectra of the SM and the CM lattices respectively. The splitting behaviours between the main subbands are different from each other. In the SM lattice the first subband shifts to the lower energy region, whereas the first two subbands shift to the lower energy region in the CM lattice. From the study of any (n, m) pairs of the lattices we know that for the SM series only the first subband shifts to the lower energy region while others shift to the higher energy region, and for the CM series the first m subbands shift to the lower energy region. These behaviours are closely related with the geometries of the lattices. As mentioned previously, the letter B in the SM series always exists in isolation regardless of the value of n, and these isolated B letters form a subband which has lowest energy due to $V_A = -V_B = V > 0$. On the other hand, the letter B in the CM series always exists in clusters consisting of m letters, and these clusters form the first m lowest bands.

3. Wavefunction and resistance

In this section we examine various wavefunctions of a kind of GF lattice, the CM lattice ($n = 1, m = 2$), in detail. To this end, one can write (1) as follows:

$$\begin{pmatrix} \psi_{n+1} \\ \psi_n \end{pmatrix} = \mathsf{M}(n) \begin{pmatrix} \psi_n \\ \psi_{n-1} \end{pmatrix} = \mathsf{M}^{(n)} \begin{pmatrix} \psi_1 \\ \psi_0 \end{pmatrix} \tag{14}$$

where the transfer matrix $\mathbf{M}(n)$ is defined by

$$\mathbf{M}(n) = \begin{pmatrix} E - V_n & -1 \\ 1 & 0 \end{pmatrix} \tag{15}$$

and

$$\mathbf{M}^{(n)} = \mathbf{M}(n)\mathbf{M}(n-1)\cdots\mathbf{M}(2)\mathbf{M}(1). \tag{16}$$

From the construction rule (2), the recursion relation for the transfer matrices $\mathbf{M}_l \equiv \mathbf{M}^{(F_l)}$ can be written as

$$\mathbf{M}_{l+1} = \mathbf{M}_{l-1}^2\mathbf{M}_l \qquad \mathbf{M}_0 = \mathbf{M}_B \quad \mathbf{M}_1 = \mathbf{M}_A \tag{17}$$

and the trace map $x_l \equiv \frac{1}{2}\mathrm{Tr}(\mathbf{M}_l)$ for the CM lattice [18,21] is given by

$$\begin{aligned} x_{l+1} &= x_l(4x_{l-1}^2 - 1) - 2x_{l-1}(2x_{l-2}^2 - 1) \\ &= x_l(4x_{l-1}^2 - 2) + \gamma \end{aligned} \tag{18}$$

where the initial conditions are

$$x_{-1} = 1 \qquad x_0 = \tfrac{1}{2}(E - V_B) \qquad x_1 = \tfrac{1}{2}(E - V_A) \tag{19}$$

and

$$\gamma = x_l - 2x_{l-1}(2x_{l-2}^2 - 1) \equiv -\tfrac{1}{2}\mathrm{Tr}(\mathbf{M}_{l-2}^{-2}\mathbf{M}_{l-1}) \tag{20}$$

is an l-independent quantity (i.e. $\gamma_{l+1} = \gamma_l$). Using the initial conditions, one can write $\gamma = x_1 - 2x_0$. When the periodic approximation with period F_l is used, the energy spectrum can be obtained from the requirement $|x_l| \leqslant 1$, and the eigenvalues under the periodic boundary condition can be obtained from $x_l = 1$.

In the trace space, there exist lots of periodic points having any cycle such as $(\pm\frac{1}{4}, \mp 1)$, $(0, \pm\frac{\sqrt{3}}{2}, \mp\frac{\sqrt{3}}{2})$, $(\pm\frac{1}{2}, \mp\frac{1}{4}, \mp 1)$, $(\pm\frac{1}{2}, \pm\frac{1}{2}, \mp 1)$, etc. There also exist points which will flow into the periodic orbits even if they do not belong to the periodic orbit initially. For example, putting the initial conditions $(x_0, x_1) = (0, \pm\frac{1}{2})$ or $(\pm\frac{1}{4}, 0)$ yields 3-cycle points $(\pm 1, \mp\frac{1}{2}, \mp\frac{1}{2})$ after $l = 2$. Furthermore, there can exist a fixed point that always gives an eigenenergy of any generation of the CM sequence. It occurs when $(x_0, x_1) = (0, -1)$. One can check from (18) that $x_l = 0$ and $x_{l+1} = -1$ mean $x_{l+m} = 1$ for any $m > l$. The term γ is known to play an important role in the trajectories of the trace map, and thus in the energy spectra of the system [20]. For $|\gamma| > 1$, most of the points except for the periodic points and their predecessors are known to escape to infinity in a few iterations and the surviving points gives the Cantor-like part of the spectra of quasiperiodic systems. On the other hand, for $|\gamma| < 1$, there can be infinitely many aperiodic points that never escape, and the energies corresponding to these bounded aperiodic orbits contribute to Bloch-like bands.

In the ordinary Fibonacci lattice, wavefunctions and resistances corresponding to the periodic orbit are known to exhibit self-similarity [40]. This feature is not peculiar to the ordinary Fibonacci lattice, but appears in the CM lattice when $|\gamma| > 1$ holds.

Figure 4 shows a wavefunction corresponding to 3-cycle orbit $(\frac{1}{2}, -\frac{1}{4}, -1)$. We take $E = 0$, $V_A = 0.5$ and $V_B = -1$. Successive figures (*b*) and (*c*) show the self-similarity clearly. Figure 5 shows a resistance R_N which also exhibits the self-similar peak structure. We take $E = 0.5$, $V_A = -1.5$ and $V_B = 1$ corresponding to 2-cycle orbit $(-\frac{1}{4}, 1)$. There exists a self-similarity between the system size $N = F_l$ and $N = F_{l+4}$, and the peaks increase algebraically. The 4-cycle of the self-similarity is due to the 4-cycle of the full transfer matrices, i.e. $\mathbf{M}_l = \mathbf{M}_{l+4}$ even though $x_l = x_{l+2}$. It is interesting to note that R_N is symmetric for the system size $N = F_{4l+1}$, and there exist two maximum peaks for that size. The peak points are located at $N_n = \sum_{k=1}^{2n} F_{2k-1} (= 6, 112, 1818, \cdots)$ and $\sum_{k=1}^{2n} F_{2k} - 2 (= 12, 226, 3640, \cdots)$. Setting $R_N \sim N^{2\beta}$, we obtain the exponent $\beta \approx 0.3677$ for these peak points. Thus the scaling transformation of the self-similar peak structure can be written as $N \to N\sigma_C^4$ and $R_N \to \Lambda^2 R_N$, where $\Lambda = \sigma_C^{4\beta}$.

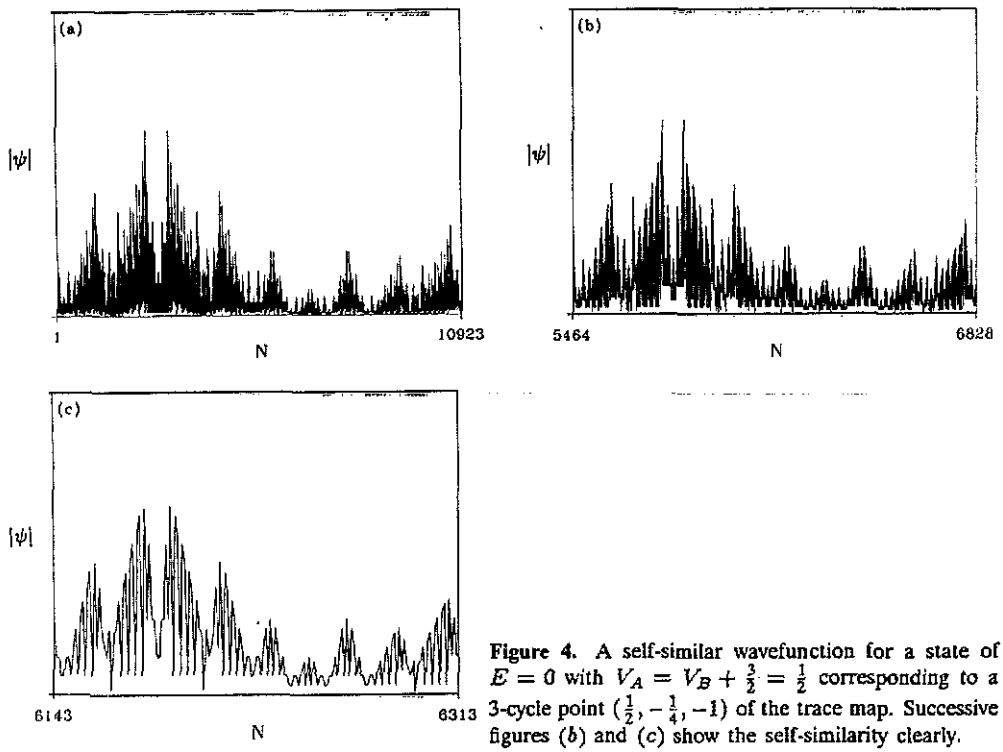

Figure 4. A self-similar wavefunction for a state of $E = 0$ with $V_A = V_B + \frac{3}{2} = \frac{1}{2}$ corresponding to a 3-cycle point $(\frac{1}{2}, -\frac{1}{4}, -1)$ of the trace map. Successive figures (*b*) and (*c*) show the self-similarity clearly.

Non-self-similar wavefunctions correspond to the aperiodic orbits of the trace map, and the existence of infinitely many orbits makes this type of the wavefunctions dominate in the CM lattice. Figure 6 shows an example of chaotic wavefunctions for the system of $V_A = V_B = 0.6$, $N = 5461 (l = 13)$ and $E = 1.402\,118\,107\,741\,281\,210$, which is an eigenvalue $(x_{l=13} = 1)$ under the periodic boundary condition. The bandwidth ΔE containing this eigenvalue is $\Delta E \sim 2.65 \times 10^{-6}$, which is somewhat smaller than that of the extended states. As shown in the figure, there is no apparent scaling.

Using the Hamilton–Cayley theorem, one can deduce the kth power of a 2×2 unimodular matrix M as follows:

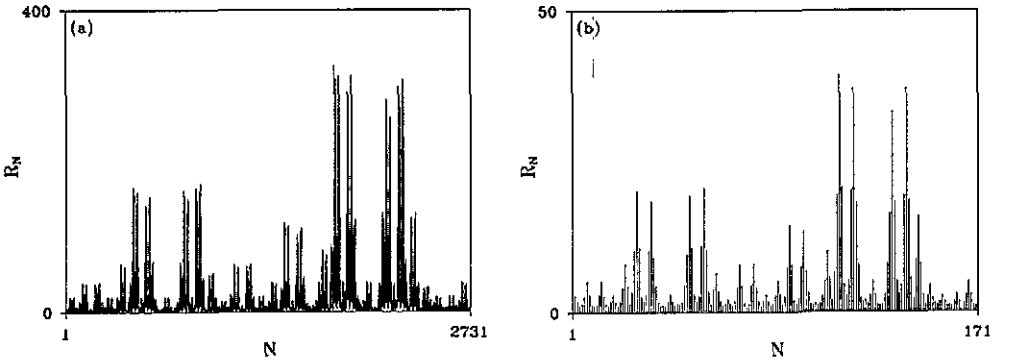

Figure 5. N dependence of R_N for a state of $E = 0.5$ with $V_A = -1.5$, $V_B = 1$ corresponding to a 2-cycle point $(-\frac{1}{4}, 1)$ of the trace map for (a) $N = 2731 (l = 12)$ and (b) $N = 171 (l = 8)$. The self-similarity between (a) and (b) is clearly shown.

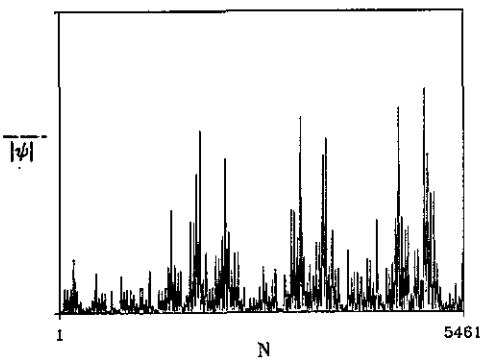

Figure 6. A chaotic wavefunction for a state of $E = 1.402\,118\,107\,741\,281\,210$ with $V_A = -V_B = 0.6$ and $l = 13 (N = 5461)$.

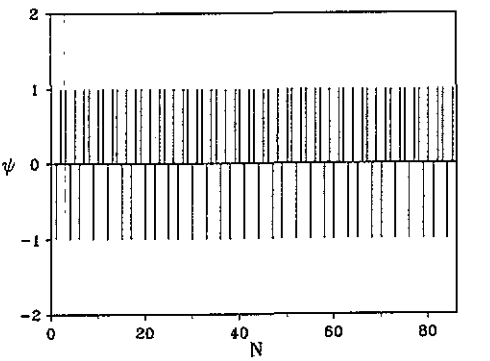

Figure 7. A wavefunction for a state of $E = -1$ with $V_A = -V_B = 1$ when the periodic boundary condition is imposed.

$$\mathbf{M}^k = C_k(m)\mathbf{M} - C_{k-1}\mathbf{I} \tag{21}$$

where $\mathbf{I}$ is the unit matrix, and $C_k(m)$ is a polynomial of $m \equiv \mathrm{Tr}(\mathbf{M})$ (a Chebychev polynomial of the second kind) which satisfies the recursion relation

$$C_{k+1}(m) = mC_k(m) - C_{k-1}(m) \tag{22}$$

with $C_1(m) = 1$ and $C_2(m) = m$. When $|m| \leqslant 2$, the kth polynomial is given by

$$C_k(m) = \frac{\sin(kx)}{\sin(x)} \qquad x = \cos^{-1}(\tfrac{1}{2}m). \tag{23}$$

Using the above equations we examined two typical examples of wavefunctions where the initial condition (x_0, x_1) satisfies $|\gamma| \leqslant 1$. The first example is a wavefunction corresponding to $(x_0, x_1) = (0, -1)$, and thus $|\gamma| = 1$ which is the critical value whether or not the Bloch-like spectrum can exist in the limit of a system of infinite size. As previously mentioned, the initial condition gives a fixed point

$x_l = 1 (l \geqslant 2)$ and the corresponding energy gives an eigenvalue of the system. It is located at the edge of the second main subband in the energy spectrum. Combining the initial condition with (19) leads to $\mathrm{Tr}(\mathsf{M}_B) = 0$ and $\mathrm{Tr}(\mathsf{M}_A) = -2$, which results in

$$C_k(B) = \sin(\tfrac{1}{2}k\pi) \qquad C_k(A) = (-1)^{k+1}k. \tag{24}$$

Thus one can write

$$\mathsf{M}_B^2 = -\mathsf{I} \qquad \mathsf{M}_A^k = (-1)^{k+1}[k\mathsf{M}_A + (k-1)\mathsf{I}]. \tag{25}$$

The relation $\mathsf{M}_B^2 = -\mathsf{I}$ allows $\mathsf{M}^{(n)}$ to have a form of M_A^k or $\mathsf{M}_B\mathsf{M}_A^k$ (neglecting signs) where $1 \leqslant k \leqslant n$. For example, $\mathsf{M}^{(2)} = \mathsf{M}_B\mathsf{M}_A$, $\mathsf{M}^{(3)} = -\mathsf{M}_A$, $\mathsf{M}^{(4)} = -\mathsf{M}_A^2$, $\mathsf{M}^{(5)} = -\mathsf{M}_A^3$, etc. In particular, for $k = F_l$

$$\mathsf{M}^{(F_l)} = -\mathsf{M}_A^{F_l-1} = \begin{pmatrix} F_{l-1}+1 & F_{l-1} \\ -F_{l-1} & -F_{l-1}+1 \end{pmatrix}. \tag{26}$$

The periodic boundary condition $\psi_{F_l} = \psi_0$ together with (14) and (26) gives rise to the relation

$$\psi_1 = -\psi_0 \tag{27}$$

regardless of l, and thus the strengths of the probability amplitude at any site can be determined. When $\mathsf{M}^{(n)}$ has a form of M_A^k,

$$\begin{aligned} |\psi_n| &= |(\mathsf{M}_A^k)_{21}\psi_1 + (\mathsf{M}_A^k)_{22}\psi_0| \\ &= |(-1)^{k+2}k\psi_0 + (-1)^{k+2}(k-1)\psi_0| \\ &= |\psi_0|. \end{aligned}$$

Similarly $|\psi_n| = |\psi_0|$ holds when $\mathsf{M}^{(n)}$ has a form of $\mathsf{M}_B\mathsf{M}_A^k$, and thus the wavefunction corresponding to the fixed point is extended with equal strength of the probability amplitude at any site, as shown in figure 7. We take $E = -1$, $V_A = -V_B = 1$ and $\psi_0 = 1$. The sign of the probability amplitude is closely related to the lattice geometry. That is, $\psi_n = 1$ when n is on the sites of the letter B or the centre sites of the AAA cluster, while $\psi_n = -1$ when n is on the sites of the isolated letter A or on the edge sites of the AAA cluster, as can be seen in the figure. Note that the state corresponding to the fixed point is very sensitive to the boundary condition. The extended wavefunction with constant probability amplitude is the result of the periodic boundary condition. When one imposes other kinds of boundary conditions, the shape of the wavefunction changes considerably. This is because the (1,1) and (1,2) (or (2,1) and (2,2)) components of M_A^k in (25) contribute to the monotonic change of the wavefunction when $\psi_1 \neq -\psi_0$. The effect of boundary conditions also clearly appears in the resistance. Figures 8(*a*) and (*b*) show the resistances for the wavenumber of the incident wave $K = \pi$ and $\frac{1}{4}\pi$ respectively. (The former is equivalent to the periodic boundary condition, i.e. $\psi_1 = -\psi_0$, while the latter is not.) The algebraically localized behaviour in figure 8(*b*) is clearly shown. From the plot of $\log R_N$ against $\log N$ we obtained $R_N \sim N^{2\tilde{\beta}}$ with an exponent $\tilde{\beta} \simeq 1.00$ for the algebraically localized state, which is a feature

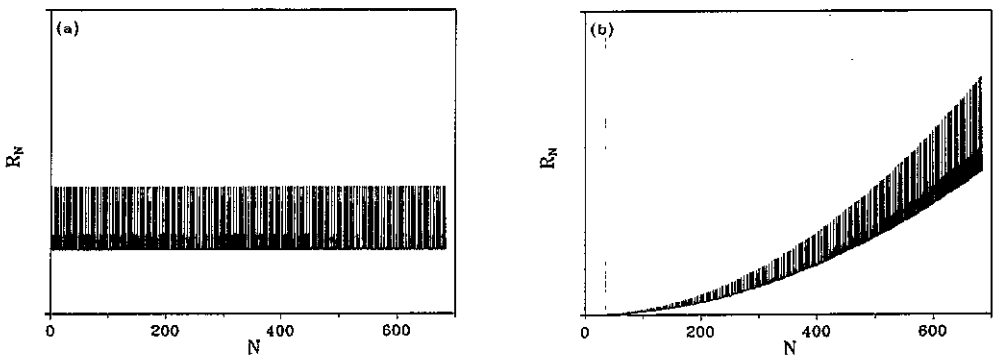

Figure 8. N dependence of R_N when the wavenumber of the incident wave is (a) $K = \pi$ and (b) $K = \frac{\pi}{4}$. The parameters are the same as in figure 7; (a) shows extended behaviour while (b) exhibits algebraically localized behaviour.

qualitatively similar to band-edge states in the periodic system and the state of a kind of fixed point in the hierarchical system [15].

The second example is a wavefunction corresponding to $(x_0, x_1) = (0, \frac{\sqrt{3}}{2})$. In this case, the trace map has a 3-cycle orbit $(0, \frac{\sqrt{3}}{2}, \frac{-\sqrt{3}}{2})$ and $|\gamma| < 1$, which means that the energy belongs to a Bloch-like spectrum. In this case

$$C_k(B) = \sin(\tfrac{1}{2}k\pi) \qquad C_k(A) = 2\sin(\tfrac{1}{6}k\pi) \qquad \mathbf{M}_B^2 = -\mathbf{I} \tag{28}$$

and

$$\mathbf{M}_A^k = \begin{pmatrix} \sqrt{3}C_{k-1}(A) - C_{k-1}(A) & C_k(A) \\ -C_k(A) & C_{k-1}(A) \end{pmatrix}. \tag{29}$$

Note that $\mathbf{M}_B^2 = -\mathbf{I}$ allows $\mathbf{M}^{(n)}$ to have the same form as that in the fixed-point case. Applying the periodic boundary condition leads to the following relation between ψ_1 and ψ_0:

$$\psi_1 = \frac{C_{F_{l-1}-1} - 1}{C_{F_{l-1}}}\psi_0. \tag{30}$$

Explicitly, $\psi_1 = \pm\psi_0, (\sqrt{3} \pm 1)\psi_0$ and $[(\sqrt{3} \pm 1)/2]\psi_0$ depending on the l of the periodic approximant F_l. From (28) and (29), one can also check that $|\psi_n|$ has only three kinds of values for any case of the relation between ψ_1 and ψ_0. For example, when the periodic approximant F_l with $l = 4 \bmod 6$ is applied, $|\psi_n|$ takes one of the values $\{1, \sqrt{3} - 1, 2 - \sqrt{3}\}$ as shown in figure 9. (We set $\psi_0 = 1$.) Thus the wavefunction having periodic orbits exhibits extended behaviour rather than self-similar behaviour, in contrast with that for the case $|\gamma| > 1$. Figure 9 shows that the sign and the probability amplitude of the wavefunction are rather chaotic in comparison with those of the fixed point. Note that imposing another kind of boundary condition does not change the property of the state, unlike that of the fixed point. This is because each component of $\mathbf{M}_A^k$ in (26) does not increase, but changes

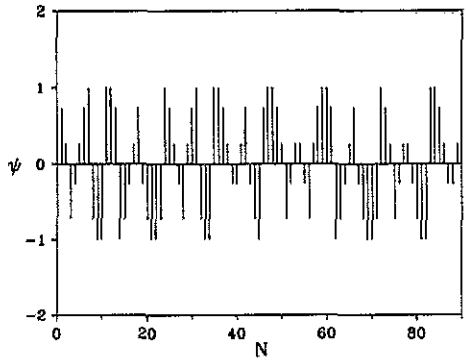

Figure 9. An extended wavefunction for a state of $E = \sqrt{3}/2$ with $V_A = V_B - \sqrt{3} = -\sqrt{3}/2$ corresponding to a 3-cycle point $(0, \sqrt{3}/2, -\sqrt{3}/2)$ of the trace map.

sinusoidally as k increases, and the wavefunction always shows extended behaviour irrespective of the relation between ψ_1 and ψ_0.

That the randomness of the CM series is intermediate between the ordinary Fibonacci and disordered lattices suggests the possibility of the localization of the wavefunctions, and the existence of localized wavefunctions has been reported for some models in GF lattices. Using the off-diagonal model, Gumbs and Ali [18] and You *et al* [32] have reported the existence of localized wavefunctions, and Severin and Riklund [23] have reported localized wavefunctions in the nickel-mean lattice. However, we think that the localization of the wavefunction is a feature of the finite size of the system, i.e. the periodic-approximation effect, at least for the present model as discussed below. Like the above authors, we also obtained strongly localized wavefunctions for a certain approximated system. Figure 10(a) shows such a wavefunction obtained for the system with $V_A = -V_B = 0.6$, $N = 2731$ ($l = 12$) and $E = 1.257\,678\,358\,452\,100\,007$. This energy corresponds to $x_{l=12} = 1.0$ and an exact eigenvalue of the system. The bandwidth is $\Delta E \sim 8.67 \times 10^{-14}$, which is very much more narrow than that of figure 9. However, the situation becomes quite different when the size of the system changes, as shown in figure 10(b). Note that the gross band structure becomes unchanged in the E–l plane irrespective of the system size, and the eigenvalues increasing with generation only fill the band regions, avoiding the gap regions which are already fixed in the previous generations [6]; the exact eigenvalues can be easily obtained from the trace map. These enable us to trace the subsequent eigenvalues and bandwidths as l changes, and we obtain the results that can be summarized as follows.

As l changes from 12 to 13, 14, 15, 16, ..., (i) the number of the eigenvalues and subbands changes to 1, 3, 5, 11, ... (Note that the CM Fibonacci numbers are 1, 1, 3, 5, 11, ...) (ii) The bandwidth ΔE changes to 4.33×10^{-14}, 3.34×10^{-14}, 2.04×10^{-14}, ...

Figure 10(b) shows an example of the subsequent eigenvalues ($l = 13$). The eigenvalue is $E = 1.257\,678\,358\,452\,001\,899$, which is slightly different from that of figure 10(a). The appearance of an additional wavepacket is clearly shown. We also tested other subsequent eigenvalues, and obtained the result that the number of the wave packets in the subsequent generation increases two times as that in the previous generation. We repeated the same analysis for different energies E showing localized wavefunctions for a certain l and obtained results similar to the above

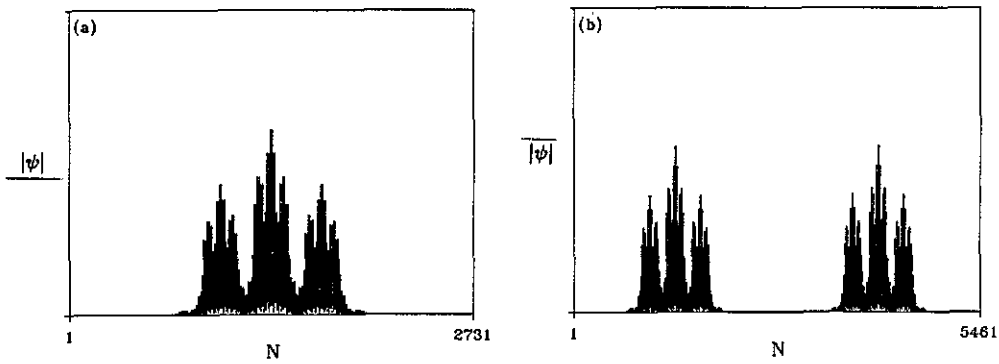

Figure 10. Wavefunctions with a strong degree of spatial localization. $V_A = -V_B = 0.6$. (*a*) $E = 1.257\,678\,358\,452\,100\,007$, $l = 12$ and (*b*) $E = 1.257\,678\,358\,452\,001\,900$, $l = 13$.

ones. This clearly shows that the appearance of spatially localized wavefunctions as in figure 10(a) is a feature of the lth approximated periodic system, and that one cannot tell the existence of localized states in the limit of infinite system size. The appearance of additional wavepackets seems to be closely related to the geometry of the lattice.

The relation of the size of the system between the lth and $(l+1)$th generation sequences is $F_{l+1} = 2F_l \pm 1$, and the ending block of the system with F_{l+1} letters is either BB or A depending on whether l is odd or even. Note that if we replace the ending block $BB(A)$ by $A(BB)$, the size of the system with F_{l+1} letters becomes exactly twice as large as that with F_l letters and the arrangement of the lattice becomes twofold, i.e. $S_{l+1} = S_l S_l$. It reminds us of the periodic arrangement of the sequence. In the case of figure 10, if we set $S = S_{l=12}$ and $S' = S$ with the ending block A replaced by BB, the lattice becomes

$$S \to SS' \to SS'SS \to SS'SSSS'SS' \to SS'SSSS'SS'SS'SSSS'SS \to \cdots.$$

In fact, S' is approximately equal to S for large l, and thus the electron feels a periodic potential with a unit cell S, which results in the appearance of recurrent wavepackets. This suggests that the localized states are not allowed in the CM lattice [29]†.

We also performed a multifractal analysis [41] on the wavefunctions. The multifractal method is known to be effective in characterizing wavefunctions, and thus it has been applied to characterizing wavefunctions in various systems [7, 8, 16, 44–46]. Recently, it has also been applied to characterizing wavefunctions under electric fields in the hierarchical [17] and the incommensurate [47] systems. Defining the partition function $Z(q, l)$ and an exponent $\tau(q)$ as

† We recently found similar behaviour in the Thue–Morse lattice. States with a localized wavepacket in a certain length show additional wavepackets as the size of the system increases, and the wavefunctions are classified into various types depending on the clustering types of the lattice elements. In [41] we refer to them as *lattice-like* wavefunctions. After the submission of this paper we were kindly informed of a reference [42] dealing with the Soucoulis–Economou model where extended states were reported which appear as 'localized' if the system size is not large enough.

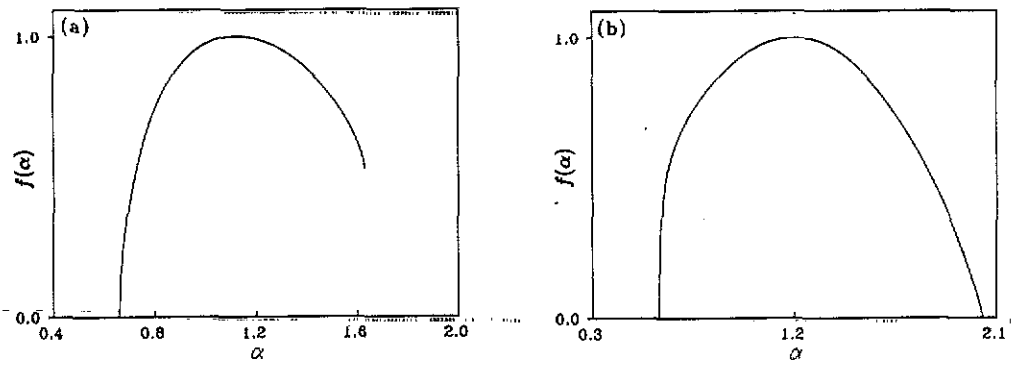

Figure 11. (f, α) spectra for critical states showing self-similar wavefunctions. (a) $E = 0$, $V_A = 0.5$ and $V_B = -1$. (b) $E = 0.5$, $V_A = -1.5$ and $V_B = 1$.

$$Z(q, l) = \sum_{i=1}^{N/l} [p_i(l)]^q \sim l^{\tau(q)} \tag{31}$$

one can determine $\tau(q)$ from the slopes of $\ln Z(q, l)$ against $\ln l$ plots, where $p_i(l)$ is the probability measure of finding an electron within the ith segment of size l. After making the scaling ansatz $p_i(l) \sim l^{\alpha_i}$ and assuming the density of scaling exponents to be $\Omega(\alpha)\mathrm{d}\alpha \sim l^{-f(\alpha)}\mathrm{d}\alpha$, one can obtain the multifractal spectrum (f, α), using the relations

$$\alpha(q) = \frac{\mathrm{d}\tau(q)}{\mathrm{d}q} \qquad f(\alpha(q)) = q\alpha(q) - \tau(q). \tag{32}$$

A critical wavefunction has a nonlinear $\tau(q)$, and thus has a continuous (f, α) spectrum defined on the finite interval $[\alpha_{\min}, \alpha_{\max}]$. On the other hand, an extended wavefunction has $(f, \alpha) = (1, 1)$, and a localized wavefunction has $(f, \alpha) = (0, 0)$ and $(1, \infty)$.

The results of the analysis on the critical wavefunctions are shown in figure 11. Figure 11(a) corresponds to the state having a 3-cycle orbit of the trace map. One can see that $f(\alpha_{\min}) = 0$ and $f(\alpha_{\max}) \neq 0$. Note that the procedure we take in calculating $\tau(q)$ is very accurate for small values of $|q|$, but there exist large fluctuations in the $\ln Z(q, l)$ against $\ln l$ plot for large values of $|q|$ and thus it becomes inaccurate to fit a straight line. We therefore tried to obtain the (f, α) spectrum in the region of the values of $|q|$ where the accuracy is good. In the calculation we found that $f(\alpha)$ easily goes to zero with increasing values of q in the positive region, while it is hardly variable under some values of q in the negative region. On this basis, we conjecture that $f(\alpha_{\min}) = 0$ and $f(\alpha_{\max}) \neq 0$. Thus we expect that the set of points having largest $p_i(l)$ goes to a single point, while the set of points having smallest $p_i(l)$ does not, since the maximum and minimum values of α correspond to the minimum and maximum values of $p_i(l)$, respectively. Recently Fujiwara *et al* [8] have calculated the (f, α) spectrum for the states of the ordinary Fibonacci lattice and argued that $f(\alpha_{\min}) \neq 0$ and $f(\alpha_{\max}) = 0$ are general properties of critical wavefunctions. However our result does not follow their argument, and their argument seems to hold only for the ordinary Fibonacci lattice. Note that similar behaviours can be found in the Haper model [46].

Figure 11(b) corresponds to the state having a 2-cycle orbit of the trace map. In contrast with the case of figure 11(a), we found that $f(\alpha)$ goes rapidly to zero in the negative-q region and not so rapidly in the positive-q region. However, the rapidity in figure 11(b) is better than that in figure 11(a) with increasing and decreasing values of q, and we obtained $f(\alpha_{\min}) = f(\alpha_{\max}) = 0$ as in the case of the band centre state of the ordinary Fibonacci lattice [7].

4. Summary

We have studied the electronic properties of GF lattices by means of the negative-eigenvalue theorem, the Landauer formula and a multifractal method. The DOS and the V dependence of energy spectra for silver-mean (SM) and copper-mean (CM) series clearly show distinctive features, which are closely related to the geometrical characteristics. The allowed states of the CM lattice were investigated in detail, and the scaling properties of the critical states were demonstrated. In contrast with the SM series, extended states exist in the CM lattice. There also exists an algebraically localized state in a certain case. However, we found that states with a strongly localized wavefunction for a given l exhibit additional wavepackets as l increases, which is closely related to the geometrical characteristics of the CM lattice. This behaviour of the wavefunctions implies the absence of strongly localized states in the CM lattice. We also performed a multifractal analysis on the critical wavefunctions, in particular on the self-similar wavefunctions, to obtain (f, α) spectra.

Acknowledgments

G Y Oh would like to thank the International Centre for Theoretical Physics, where part of the work was motivated. The authors also thank the referees for constructive suggestions. This work was supported in part by the Scientific Research Centre through the Centre for Theoretical Physics in Seoul National University.

References

[1] Shechtman D, Blech I, Gratias D and Cahn J W 1984 *Phys. Rev. Lett.* **53** 1951
[2] Kohmoto M, Kadanoff L P and Tang C 1983 *Phys. Rev. Lett.* **50** 1870
Ostrund S, Pandit R, Rand D, Schellnhuber H J and Siggia E 1983 *Phys. Rev. Lett.* **50** 1873
[3] Niu Q and Nori F 1986 *Phys. Rev. Lett.* **57** 2057
[4] Ashraff J A and Stinchcombe R B 1988 *Phys. Rev.* B **37** 5723
[5] Liu Y and Sritrakool W 1991 *Phys. Rev.* B **43** 1110
[6] Fujita F and Machida K 1986 *Solid State Commun.* **59** 61
[7] Evangelou S N 1987 *J. Phys. C: Solid State Phys.* **20** L295
[8] Fujiwara T, Kohmoto M and Tokihiro T 1989 *Phys. Rev.* B **40** 7413
[9] Sutō A 1989 *J. Stat. Phys.* **56** 525
[10] Merlin R, Bajema K, Clarke R, Juang F Y and Bhattacharya P K 1985 *Phys. Rev. Lett.* **55** 1768
[11] Axel F, Allouche J P, Kléman M, Mendès-France M and Peyrière J 1986 *J. Physique Coll.* **47** C3 181
[12] Aubry S, Godrèche C and Luck J M 1987 *Europhys. Lett.* **4** 639
[13] Luck J M 1989 *Phys. Rev.* B **39** 5834
[14] Bellissard J, Bovier A and Ghez J M 1991 *Commun. Math. Phys.* **135** 379
[15] Würtz D, Schneider T, Politi A and Zannetti M 1989 *Phys. Rev.* B **39** 7829

[16] Roman H E 1987 *Phys. Rev.* B **36** 7173
[17] Oh G Y, Ryu C S and Lee M H 1992 *Phys. Rev.* B **45** 6400
[18] Gumbs G and Ali M K 1988 *Phys. Rev. Lett.* **60** 1081; 1988 *J. Phys. A: Math. Gen.* **21** L517; 1989 *J. Phys. A: Math. Gen.* **22** 951
[19] Holzer M 1988 *Phys. Rev.* B **38** 1709; 1988 *Phys. Rev.* B **38** 5756
[20] Kolář M and Ali M K 1989 *Phys. Rev.* A **39** 6538
[21] You J Q and Yang Q B 1990 *J. Phys.: Condens. Matter* **2** 2093
[22] Severin M and Riklund R 1989 *J. Phys.: Condens. Matter* **1** 5607
[23] Severin M and Riklund R 1989 *Phys. Rev.* B **39** 10362
[24] Chakrabarti A and Karmakar S N 1991 *Phys. Rev.* B **44** 896
[25] Kolář M and Ali M K 1990 *Phys. Rev.* B **41** 7108; 1989 *Phys. Rev.* B **39** 426
[26] Kalugin P A, Kitaev A Yu and Levitov L S 1986 *Zh. Eksp. Teor. Fiz.* **91** 692
[27] Ali M K and Gumbs G 1988 *Phys. Rev.* B **38** 7091
[28] Dulea M, Severin M and Riklund R 1990 *Phys. Rev.* B **42** 3680
[29] Severin M, Dulea M and Riklund R 1989 *J. Phys.: Condens. Matter* **1** 8851
Miyazaki H and Inoue M 1990 *J. Phys. Soc. Japan* **59** 2563
[30] Queffélec M 1987 *Substitution Dynamical Systems: Spectral Analysis (Lecture Notes in Mathematics 1294)* (Berlin: Springer)
[31] Burrows B L and Sulston K W 1991 *J. Phys. A: Math. Gen.* **24** 3979
[32] You J Q, Yan J R, Xie T, Zeng X and Zhong J X 1991 *J. Phys.: Condens. Matter* **3** 7255
[33] Aviram I 1987 *J. Phys. A: Math. Gen.* **20** 1025
de Bruijn N G 1981 *Proc. Kon. Nederl. Acad. Wetensch.* A **84** 27
[34] Odagaki T and Aoyama H 1988 *Phys. Rev. Lett.* **61** 775
[35] Dean P 1972 *Rev. Mod. Phys.* **44** 127
[36] Landauer R 1970 *Phil. Mag.* **21** 863
Stone A D, Joannopoulos J D and Chadi D J 1981 *Phys. Rev.* B **24** 5583
[37] Wijnands F 1989 *J. Phys. A: Math. Gen.* **22** 3267
[38] Oh G Y, Ryu C S and Lee M H *Phys. Rev.* B submitted
[39] Qin M G, Ma H R and Tsai C H 1990 *J. Phys.: Condens. Matter* **2** 1059
[40] Schneider T, Politi A and Würtz D 1987 *Z. Phys.* B **66** 469
[41] Ryu C S, Oh G Y and Lee M H 1992 *Phys. Rev.* B **46** at press
[42] Wieko C and Roman E 1984 *Phys. Rev.* B **30** 1603
[43] Halsey T C, Jensen M H, Kadanoff L P, Procaccia I and Shraiman B I 1986 *Phys. Rev.* A **33** 1141
[44] Pietronero L, Siebesma A P, Tosatti E and Zannetti M 1987 *Phys. Rev.* B **36** 5635
[45] Siebesma A P and Pietronero L 1987 *Europhys. Lett.* **4** 597
[46] Hiramoto H and Kohmoto M 1989 *Phys. Rev.* B **40** 8225
[47] Ryu C S, Oh G Y and Lee M H 1992 *J. Phys.: Condens. Matter* **4** at press